



Biological effects of a complex of vanadium(V) with salicylaldehyde semicarbazone in osteoblasts in culture: Mechanism of action

Josefina Rivadeneira^{a,b}, Daniel A. Barrio^a, Gabriel Arrambide^c, Dinorah Gambino^c,
Liliana Bruzzone^d, Susana B. Etcheverry^{a,b,*}

^a Cátedra de Bioquímica Patológica, Facultad de Ciencias Exactas, UNLP, 47 y 115 1900 La Plata, Argentina

^b CEQUINOR (CONICET-UNLP), Facultad de Ciencias Exactas, UNLP, La Plata, Argentina

^c Facultad de Química, Universidad de la República, Montevideo, Uruguay

^d Departamento de Química, Facultad de Ciencias Exactas, UNLP, La Plata, Argentina

ARTICLE INFO

Article history:

Received 1 September 2008

Received in revised form 14 November 2008

Accepted 18 November 2008

Available online 28 November 2008

Keywords:

Vanadium
Semicarbazones
Osteoblasts
Cytotoxicity
Oxidative stress
Actin fibers

ABSTRACT

Vanadium compounds display important pharmacological actions *in vivo* and *in vitro* systems. Semicarbazones are versatile ligands with therapeutic effects. Herein, we report the effects of V^VO₂(salicylaldehyde semicarbazone) (V(V)-Salsem) on two osteoblast cell lines in culture (MC3T3-E1 and UMR106). V(V)-Salsem inhibited cell proliferation in a dose response manner. At 100 μM, the complex caused an inhibition of ca. 48% and 38% for the normal and the tumoral osteoblasts, respectively ($p < 0.001$). This inhibition could be partially reversed to 35% and 28% by NAC (N-acetylcysteine) and a mixture of vitamins E and C. Changes in cell proliferation correlated with morphological alterations and the disruption of actin cytoskeleton fibers. The complex also enhanced the level of ROS (reactive oxygen species) up to ca. 100% over basal in both cell lines. Activation of ERK signalling cascade was also observed. These events led to apoptosis (up to 44% in MC3T3-E1 and 33% in UMR106 cells). Scavengers of ROS and inhibitors of ERK cascade allowed to elucidate the mechanisms involved in the cytotoxicity. In conclusion, V(V)-Salsem displayed cytotoxic effects on osteoblasts in culture through the production of free radicals and the activation of ERK cascade. These mechanisms triggered the apoptotic events that conveyed to cell death.

© 2008 Elsevier Inc. All rights reserved.

1. Introduction

Semicarbazones are versatile compounds of considerable interest because of their chemistry and potentially beneficial biological activities, such as antitumoral, antibacterial, antiviral and antimalarial effects [1]. The biological activities of these ligands are considered to be related to their ability to form chelates with metals. Biological actions of metal complexes differ from those of either ligands or metal ions, and increased or decreased biological activities are reported for several transition metal complexes.

Vanadium is a widespread trace element distributed in nature [2]. In higher animals, once absorbed through the gastrointestinal tract, it is mainly accumulated in bone tissue [3]. In the last decades, vanadium compounds have been widely studied because their potential therapeutic applications. The pharmacological effects of vanadium include insulin mimetic actions [4,5], antineoplastic effects [6,7] and osteogenic effects [8–10].

In particular, the antitumoral actions of vanadium can be determined through a deleterious effect on tumoral cell proliferation and differentiation as well as on cellular morphological alterations [11]. Previous experimental data support the hypothesis that vanadium compounds exert their antitumoral effects through different mechanisms such as the induction of tyrosine residues phosphorylation, mainly due to the inhibition of key protein tyrosin phosphatases (PTPases), which in turn promote the activation of the extracellular regulated kinase (ERK) pathway [12,13]. Moreover, other putative mechanisms of actions which have been considered are: changes in cell cytoskeleton proteins [14] as well as an increment in the oxidative stress (production of reactive oxygen species, ROS) [15,16], alterations in the intracellular concentration of reduced glutathione (GSH) [17,18], induction of apoptosis [11], as well as diverse effects on DNA synthesis and breakdown have also been described as putative mechanisms of action [19,20].

On the other hand, it has been reported that vanadium can also cause toxic actions in living systems [21,22]. To understand the toxicity of vanadium compounds it is essential to know the mechanisms of action as well as the susceptibility of different cells to these compounds.

In the frame of a project devoted to the synthesis of vanadium derivatives with pharmacologically active ligands, a complex of

* Corresponding author. Address: Cátedra de Bioquímica Patológica, Facultad de Ciencias Exactas, UNLP, 47 y 115 (1900) La Plata, Argentina. Tel.: +54 221 423 5333x49; fax: +54 221 425 9485.

E-mail address: etcheverry@biol.unlp.edu.ar (S.B. Etcheverry).

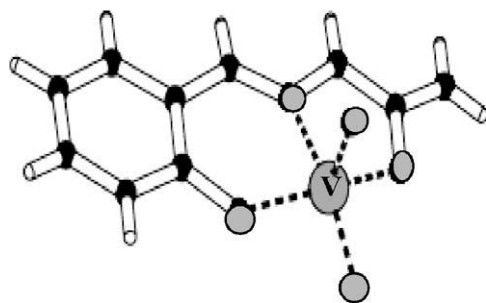


Fig. 1. Structure of V(V)-Salsem. Vanadium and oxygen atoms in grey.

vanadium(V) with salicylaldehyde semicarbazone (V(V)-Salsem) (Fig. 1), has been previously reported [23].

Fig. 1 shows the structure of this complex solved by X-ray diffraction methods. The vanadium ion is in a distorted square-pyramidal environment. It is coordinated at the pyramid basis to a salicylaldehyde semicarbazone molecule, that acts as a tridentate ligand through its azomethine nitrogen atom and its carbonyl and deprotonated phenol oxygen atoms, and to an oxo ligand. The fivefold coordination is completed by another oxo ligand at the pyramid apex.

In the present study we investigate the bioactivity of this complex in osteoblast-like cells in culture, focusing the attention on its cytotoxicity effects and the elucidation of its mechanisms of action.

2. Materials and methods

V(V)-Salsem was provided by Dr. Dinorah Gambino and synthesized according to previously reported results [23]. Tissue culture materials were purchased from Corning (Princeton, NJ, USA), Dulbeccó's Modified Eagles Medium (DMEM), and trypsin-ethylenediaminetetraacetic acid (EDTA) from Gibco (Gaithersburg, MD, USA), and fetal bovine serum (FBS) from GBO SA (Argentina). Electrochemical luminescence (ECL) kit was provided by Amersham (LIFE Science). The specific antibody rabbit polyclonal IgG anti-ERK (K-23), mouse monoclonal anti-phosphorylated ERK (PERK) (E-4), anti-rabbit IgG-horseradish peroxidase (HRP) and anti-mouse IgG-HRP were purchased from Santa Cruz Biotechnology.

Dihydrorhodamine 123 (DHR) was purchased from Molecular Probes (Eugene, OR). Annexin V – Fluorescein isothiocyanate (FITC)/Propidium Iodide (PI) and Phalloidin-FITC were from Invitrogen Corporation (Buenos Aires, Argentina). All other chemical were from Sigma Chemical Co. (ST. Louis, MO).

Fresh stock solutions of the complex and the free ligand were prepared in a mixture of free serum culture medium DMEM/Dimethyl sulfoxide (DMSO) (60:40) at 10 mM concentration and diluted in DMEM according to the concentrations indicated in the legends of the figures. Precautions should be taken with the maximum concentration of DMSO in the well plate. We used 0.4% in order to avoid toxic effects of this solvent for the osteoblasts. The stability of this complex has been previously monitored by ^1H NMR at 30 °C in DMSO- d_6 and by electronic spectroscopy and TLC at 37 °C in DMSO (1%)-buffer phosphate (pH 7.4). [23,24]. Both studies allowed discarding the formation of vanadyl species and determining the stability of the complex towards release of ligand with time, since no free ligand was detected after more than 24 h. These results showed that no vanadate could be formed since no decomposition of the complex occurred during the time involved in the biological manipulations and experiments.

2.1. Cell culture

MC3T3-E1 osteoblastic mouse calvaria-derived cells and UMR106 rat osteosarcoma-derived cells were grown in DMEM

supplemented with 100 U/ml penicillin, 100 $\mu\text{g}/\text{ml}$ streptomycin and 10% (v/v) fetal bovine serum (FBS) in a humidified atmosphere of air plus 5% CO_2 at 37 °C. When 70–80% confluence was reached, cells were subcultured using 0.1% trypsin 1 mM EDTA in Ca^{2+} - Mg^{2+} free phosphate buffered saline (PBS) (11 mM KH_2PO_4 , 26 mM Na_2HPO_4 , 115 mM NaCl, pH: 7.4) [25,26]. For experiments, cells were grown in multi-well plates. When cells reached the confluence appropriate for each type of experiment, the monolayers were washed twice with DMEM and were incubated in different conditions according to the experiments.

2.2. Cell proliferation assay

A mitogenic bioassay was carried out as described by Okajima et al. [27] with some modifications. Briefly, cells were grown in 48-well plates. When cells reached 70% confluence, the monolayers were washed twice with serum-free DMEM and incubated with medium alone (basal) and different concentrations (2.5–100 μM) of the complex or the free ligand. Besides, incubations were also carried out with the complex plus N-acetylcysteine (NAC), a mixture of vitamins C and E, PD98059 and wortmannin. Cells were preincubated with the following doses of the mentioned inhibitors for different periods previous to the addition of different concentrations of the complex: NAC (100 μM for MC3T3-E1 osteoblasts and 200 μM for the tumoral osteoblasts) during 2 h, a mixture of vitamins E and C (25 μM each for MC3T3-E1 cells and 50 μM each for UMR106 cells during 6 h, PD98059 (1–20 μM) and wortmannin (0.25–10 μM) for 30 min in both cell lines. After these preincubations, 100 μM V(V)-Salsem were added for 24 h at 37 °C. After this treatment, the monolayers were washed with PBS and fixed with 5% glutaraldehyde/PBS at room temperature for 10 min. After that, they were stained with 0.5% crystal violet/25% methanol for 10 min. Then, the dye solution was discarded and the plate was washed with water and dried. The dye taken up by the cells was extracted using 0.5 ml/well 0.1 M glycine/HCl buffer, pH 3.0/30% methanol and transferred to test tubes. Absorbance was read at 540 nm after a convenient sample dilution. We previously showed that under these conditions, the colorimetric bioassay strongly correlated with cell proliferation measured by cell counting in Neubauer chamber [25,26].

2.3. Cell morphology

Cells were grown on glass coverslips and incubated with V(V)-Salsem at different doses in serum-free DMEM for 24 h. Then, the cells were fixed and stained with Giemsa [28,29]. Samples were observed under light microscopy and pictures were taken for further evaluation.

3. Mechanisms of action

3.1. Oxidative stress

Intracellular H_2O_2 was measured spectrophotometrically, using the leuco probe DHR 123 which preferentially reacts with H_2O_2 , and is oxidized to the fluorescent molecule rhodamine 123 [30,31]. Briefly, the osteoblast cell lines were incubated with V(V)-Salsem for 24 h followed by an incubation with DHR for 30 min at 37 °C. The cells were then washed in PBS and scrapped into 1 ml 0.1% Triton-X100. The cell extracts were then analyzed using an Aminco-Bowman SPF100 spectrofluorometer equipped with a Hamamatsu R928 photomultiplier tube (excitation wavelength, 490 nm; emission wavelength, 520 nm). Results were corrected for protein content, which was assessed by the method of Bradford [32].

3.2. Sensitivity to hydrogen peroxide (H₂O₂)

In order to determine if the generation of increased levels of intracellular H₂O₂ may be one of the pathways used by V(V)-Salsem to exert cytotoxicity in osteoblast-like cells, the cells were incubated for 24 h in 48-well plates at 37 °C with H₂O₂ in varying concentrations, as specified in the legends to the figures. After incubation, the cellular viability was measured by the crystal violet bioassay.

3.3. Cytoskeleton rearrangement

To visualize actin filaments, a fluorescence staining method was performed. Cells were grown on glass coverslips until a 70% of confluence. Then, they were incubated for 24 h at 37 °C with different doses of the compounds. After that, the cells were fixed, permeabilized during 4 min at room temperature using absolute ethanol (cold at –20 °C), washed with phosphate buffered saline (PBS) and blocked with 5% non-fat milk for 2 h. After washing, the cells were incubated with Phalloidin-FITC (1/300) in the blocking agent for 2 h. The samples were washed again and mounted in slides with glycerol (80%)/PBS plus PI (5 µg/ml). Labeled cells were visualized using a fluorescence microscope and pictures were taken for later evaluation.

3.4. Measurement of the exposure of phosphatidyl serine (PS) by Annexin V-FITC/PI

During apoptosis one of the first membrane changes that can be detected is the exposure of PS residues. This phospholipid reacts with Annexin V and apoptotic cells show a green fluorescence on their surface. Cells that have lost membrane integrity (necrotic cells) will have a red fluorescent nucleus stained with PI.

Surface exposure of PS by apoptotic cells was measured by adding Annexin V-FITC/PI to the culture medium following the recommendations of the manufacturer. The cells were subsequently incubated for 10 min in the dark at room temperature. The adherent cells were rinsed twice with PBS and were harvested by scrapping with a rubber policeman [33]. Cells were analyzed using a flow cytometer (BD FACS Calibur™). Four subpopulations were expected in the cytogram: the mechanically damaged vital (Annexin V–/PI+), the undamaged vital (Annexin V–/PI–), the apoptotic (Annexin V+/PI–), and the secondary necrotic (Annexin V+/PI+) subpopulations. Besides, in order to test the influence of oxidative stress on the apoptosis events, experiments were also performed in the presence of GSH at concentrations of 0.25 mM for MC3T3-E1 cells and 1 mM for UMR106 osteoblasts. Cells were preincubated with GSH for 2 h before to the addition of the complex.

3.5. Western blotting of cell lysates

UMR106 and MC3T3-E1 osteoblast-like cells were subcultured into 6-well-plates in DMEM supplemented with 100 U/ml penicillin, 100 µg/ml streptomycin and 10% (v/v) FBS at 37 °C, 5% CO₂. When 100% confluence was reached, the medium was removed and the cells were washed twice with serum-free DMEM. Cells were preincubated for 1 h in serum-free DMEM with different concentrations of the inhibitors according to the figure legends, and then, 1 mM of the complex was added and incubated at 37 °C for an additional hour. Then, the cells were washed twice with cold PBS and lysed in Laemmli buffer [34]. Protein content was determined in each lysated cellular fractions. Aliquots with equal amounts of protein were separated on 12.5% sodium dodecyl sulfate polyacrylamide gel electrophoresis (SDS–PAGE) under reducing conditions. Then, they were transferred to acetate

cellulose membranes, and examined by immunoblotting with specific antibodies against the phosphorylated (1:1000) and not phosphorylated (1:1000) ERK-1/2. Then, they were revealed by an ECL commercial kit [35].

4. Statistical methods

At least three independent experiments were performed for each experimental condition. Results are expressed as the mean ± SEM. Statistical differences were analyzed using Student's *t*-test.

5. Results

5.1. V(V)-Salsem induced cytotoxicity on osteoblast proliferation

The effect of the complex and the free ligand on the proliferation of osteoblast-like cells in culture was estimated by the crystal violet bioassay. Fig. 2 shows that at lower tested concentrations the complex did not exert any effect. Nevertheless, by increasing the concentration of V(V)-Salsem up to 100 µM, a dose-dependent decrease of cell survival could be determined. This effect was statistically significant after 10 µM for the non-transformed MC3T3-E1 cells and for 25 µM in the tumoral osteoblasts (UMR106). This observation suggests a greater sensitivity to V(V)-Salsem for the non-transformed cell line. At the highest tested concentration of 100 µM, the complex caused an inhibition of ca. 48% and 38% for the normal and the tumoral osteoblasts, respectively (*p* < 0.001). Besides, the free ligand did not display any effect on cell survival in the whole range of the tested concentrations.

In order to better evaluate the cytotoxic effect of V(V)-Salsem in osteoblasts in culture, we then analyzed its action on cell morphology by light microscopy.

5.2. Morphological changes

Taking into account the deleterious effects of the complex on the proliferation of osteoblast cell lines, we next investigated the action of this complex on the morphology of MC3T3-E1 and UMR106 cells. As can be seen from Fig. 3a, the MC3T3-E1 control

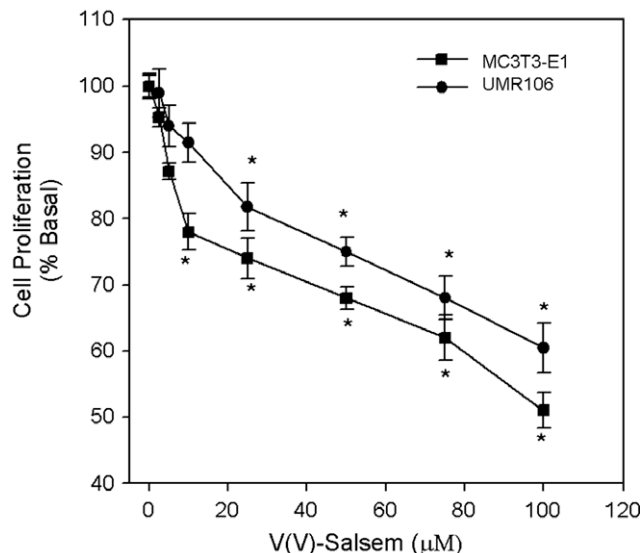


Fig. 2. Effect of V(V)-Salsem on MC3T3-E1 and UMR106 osteoblast-like-cell proliferation. Cells were incubated in serum-free DMEM alone (basal) or with different concentration of V(V)-Salsem at 37 °C for 24 h. Result are expressed % basal and represent the mean ± SEM (*n* = 9). *p* < 0.001.

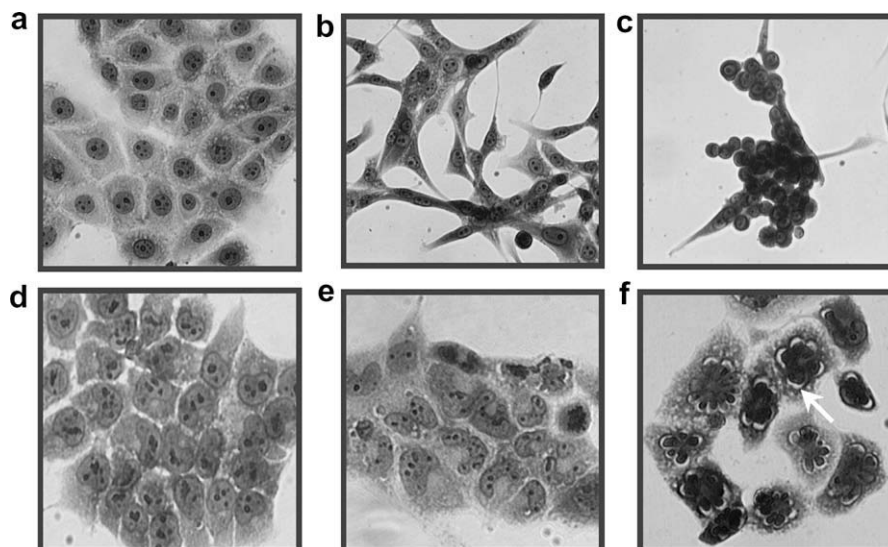


Fig. 3. Effect on cell morphology on the treatment on the osteoblast-like cells with V(V)-Salsem. Upper panel, MC3T3-E1 osteoblasts. (a) basal, (b) 10 μ M, (c) 100 μ M. Lower panel, UMR106 cells. (d) basal, (e) 25 μ M, and (f) 100 μ M. Arrow indicates membrane blebs. Obj. 100 \times .

monolayer showed the aspect of a typical fibroblast-like culture. Cells presented round nuclei, were stellate in shape and exhibited thin lamellar processes connecting each other with their neighboring. The deleterious effect of V(V)-Salsem could be observed at 10 μ M concentration (Fig. 3b). A gradual cytoplasm condensation and loss of the connections between the cells could be seen. The preosteoblasts were elongated as well as the nuclei and the cells adopted a fusiform shape. At 100 μ M concentration, most pronounced changes were observed; the nuclei were pyknotic and scarce and very thin cytoplasm connections between cells could be observed. Besides, an important number of cells died and detached from the monolayer (Fig. 3c).

The morphological characteristics of a culture of UMR106 osteosarcoma cells can be seen in Fig. 3d. These cells showed polygonal shape, well stained nuclei of irregular form and well defined cytoplasm. Cells connected with their neighbors through lamellar processes. At 25 μ M of the complex (Fig. 3e), some nuclei showed apoptotic transformations such as membrane blebs (see arrow). The morphological alterations of the nuclei were more marked as the complex concentration increased up to 100 μ M (Fig. 3f).

5.3. Alterations in cytoskeleton actin

Staining of the actin protein with Phalloidin-FITC was used to visualize cytoskeleton architecture in the osteoblast-like cells growing in the presence of different complex concentrations. Fig. 4 (upper panel) presents the organization of actin filaments in MC3T3-E1 cells without the addition of the complex (a) and treated with vanadium 10 μ M (b) and 100 μ M (c). In the control, actin microfilaments were regularly distributed and placed in the direction of the main axis of the preosteoblastic cells. In the osteoblasts exposed to the vanadium complex, actin filaments were rearranged and the shape of the cells were lost as the concentration of V(V)-Salsem increased. At 10 μ M slight modifications in the actin fiber disposition could be observed. At 100 μ M a complete disruption of cell shape could be seen. The loss of cytoplasm was especially marked and this resulted in a nuclei gathering.

Fig. 4 (lower panel) shows the characteristics of the actin filaments in UMR106 cells. Control cells (d) displayed an organized architectural disposition of the fibers in a similar pattern to that found for the MC3T3-E1 cells under basal condition. When the

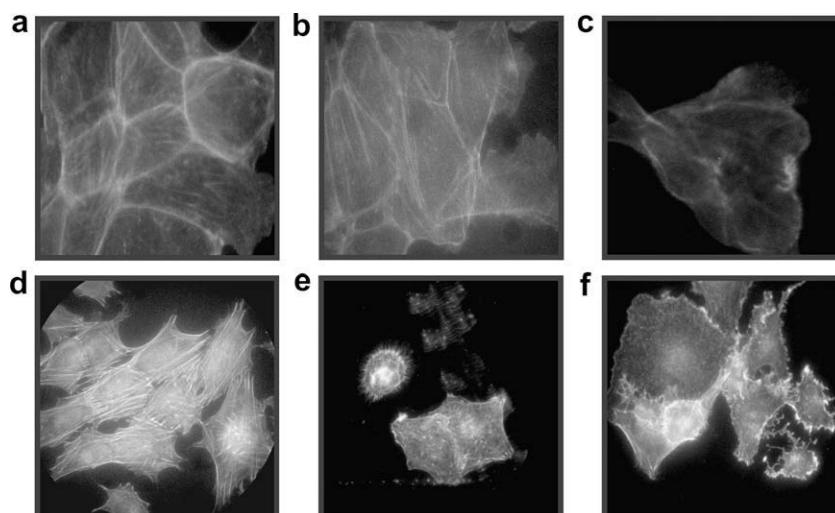


Fig. 4. Effect on actin fibers upon the treatment with V(V)-Salsem. Upper panel, MC3T3-E1 osteoblasts. (a) basal, (b) 10 μ M, (c) 100 μ M. Lower panel, UMR106 cells. (d) basal, (e) 25 μ M, and (f) 100 μ M. Obj. 100 \times .

osteosarcoma cells were exposed to different concentrations of the complex, the regularity of this pattern altered as the doses of the V(V)-Salsem increased. For these tumoral cells, the first changes in actin microfilament organization could be detected at 25 μM (e). At the highest tested dose of 100 μM (f), there was a complete disassembly of actin network, fragmentation of some nuclei and the lost of cellular membrane in some cells. These results are in accordance with the morphological alterations observed with Giemsa staining as well as with the proliferation results obtained with the crystal violet assay previously reported.

From a molecular point of view, the possible mechanisms of cell death triggered by V(V)-Salsem were investigated through the determination of the oxidative stress (ROS production), the apoptosis and the induction of the active (phosphorylated) forms of ERKs 1/2.

5.4. Oxidative stress

The determination of ROS was carried out using DHR 123. This probe is a non fluorescent compound that preferentially tested the production of H_2O_2 . In the cells, DHR 123 is oxidized to Rhodamine 123 when exposed to oxidizing agents. Cell extracts for rhodamine 123 measurements were obtained and processed as previously described, using fluorescence spectroscopy. As can be seen from Fig. 5, V(V)-Salsem induced a dose-dependent oxidative stress in both cell lines. Significant differences vs. basal could be observed from 25 μM ($p < 0.001$).

We therefore tested the sensitivity of the osteoblast cell lines to H_2O_2 . Fig. 6 shows that MC3T3-E1 and UMR106 cells were affected by the hydrogen peroxide in a dose response manner. Besides, the non tumoral osteoblasts were more sensitive towards this substance since the first statistically difference could be observed at 5 μM while in the tumoral cells it corresponded to a concentration of 10 μM .

On the bases of these results we assumed that the oxidative stress may play a key role in the toxic effect of the complex. To confirm this hypothesis we first studied the effect of NAC on the level of ROS generated by the complex in the cultures of osteoblasts. As expected, NAC diminished the oxidative stress in both cell lines

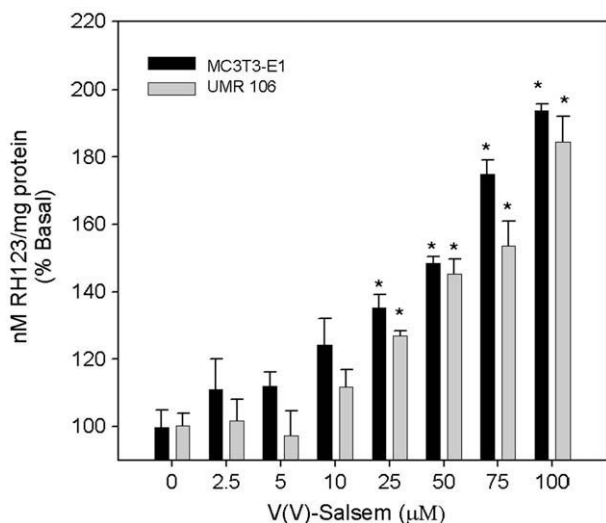


Fig. 5. Effect of V(V)-Salsem on DHR oxidation to rhodamine. Osteoblast-like cell were incubated with different concentrations of the complex for 24 h. The generation of ROS was evaluated as described in Materials and methods. Values represent the means \pm SEM, $n = 6$. Statistically significant differences vs. control are $p < 0.001$.

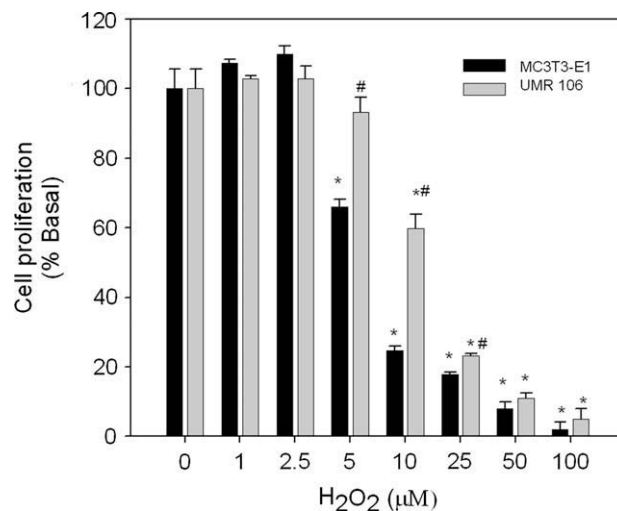


Fig. 6. Cellular sensitivity to H_2O_2 . Cells were incubated with various H_2O_2 concentrations for 24 h and the viability was measured by the crystal violet assay. The results are expressed as the percentage of basal. Values represent the means \pm SEM, $n = 6$. Statistically significant differences vs. control are $p < 0.001$. Statistically difference between cell lines are $\#p < 0.001$.

(Fig. 7a and b). Similar results were obtained with a mixture of vitamin C and E (data not shown).

Then, we evaluated the effects of the ROS scavengers on cell proliferation. The results can be seen in Fig. 8a and b. The scavengers partially reversed the vanadium cytotoxicity allowing a better survival of the osteoblasts.

5.5. Apoptosis

Apoptosis is a physiological process of cell death enhanced in the presence of injuring agents. Apoptosis determines various modifications in cell structure, mainly at the cellular membrane level. One of the first alterations that can be defined is the externalization of the PS, at the outer plasma membrane leaflet. Fig. 9a displays the quantification of apoptotic cells determined by flow cytometry in MC3T3-E1 cells incubated with different doses of V(V)-Salsem. As can be seen MC3T3-E1 cells showed 17% of apoptotic cells under basal conditions (without vanadium compound). This percentage increased to 34% at 50 μM reaching a maximum of 44% at 100 μM . In the case of tumoral osteoblasts (Fig. 9b), an increment from 14% in the control to 33% at 100 μM could be measured. Necrotic cells were observed neither in the normal nor in the tumoral osteoblasts.

Since GSH is one of the most important hydrogen peroxide scavenger, we next tested the effect of 100 μM V(V)-Salsem plus 0.25 or 1 mM GSH for MC3T3-E1 and UMR106, respectively. Under these experimental conditions, preliminary results indicated a decrease of apoptotic cells.

5.6. ERK-activation

The activation of ERK cascade by V(V)-Salsem was evaluated using the method previously described [35]. Proteins in the cell extracts were separated by SDS-PAGE and examined by immunoblotting with specific antibodies against the phosphorylated and non-phosphorylated forms of ERK-1/2. A representative immunoblot for UMR106 of the effects of the complex is shown in Fig. 10. As can be seen ERK cascade was activated by 1 mM of V(V)-Salsem, this effect was observed in both cell lines. The relative intensities of the bands pERK-1/2 to the total ERK determined

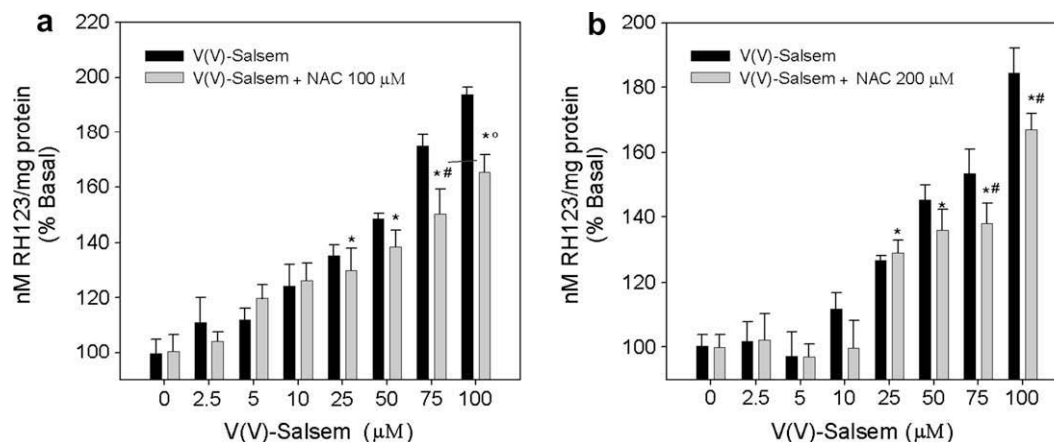


Fig. 7. Effect of V(V)-Salsem on DHR oxidation to rhodamine in presence of NAC, MC3T3-E1 cells were incubated with 100 μM of NAC plus different concentrations of the complex (a). Values represent the means \pm SEM, $n = 6$. Statistically significant are $^* p < 0.001$, when compared with the control; $^\# p < 0.05$, $^\circ p < 0.002$ when compared with the respective dose without NAC. UMR106 cells were incubated with 200 μM of NAC plus different concentration of V(V)-Salsem (b). Values represent the means \pm SEM, $n = 6$. Statistically significant are $^* p < 0.001$ when compared with control; $^\# p < 0.05$, when compared with the respective dose without NAC.

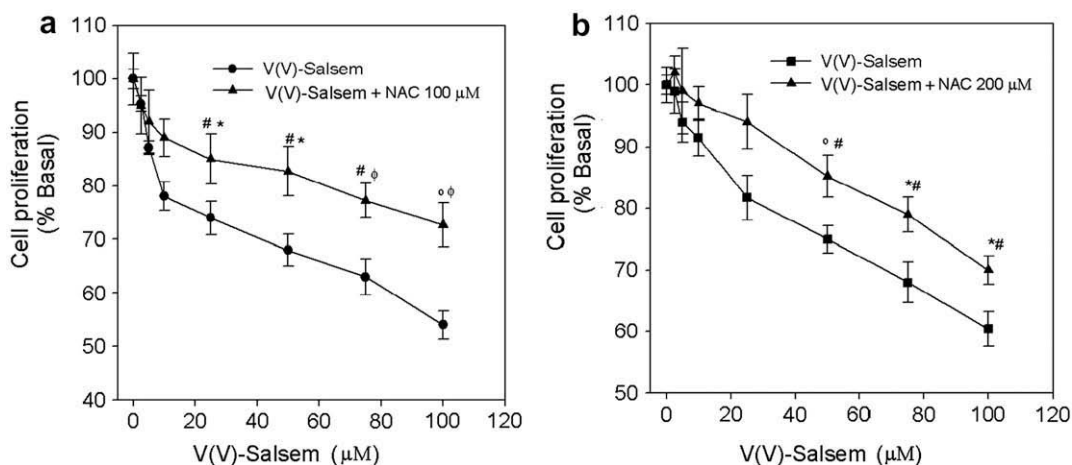


Fig. 8. Effect of V(V)-Salsem on MC3T3-E1 (a) and UMR106 (b) osteoblast-like-cell proliferation in the presence of NAC. Cells were incubated in serum-free DMEM alone (basal) or with different concentration of V(V)-Salsem plus NAC 100 μM for MC3T3-E1 or 200 μM for UMR106. Result are expressed % basal and represent the mean \pm SEM ($n = 6$). Statistically significant differences for MC3T3-E1 are $^* p < 0.05$; $^\circ p < 0.002$ when compared with control; $^\# p < 0.05$; $^\circ p < 0.002$ when compared with the corresponding dose of the complex without NAC. Statistically significant differences for UMR106 are $^* p < 0.002$; $^\circ p < 0.001$ when compared with control; $^\# p < 0.05$; $^\circ p < 0.05$ when compared with the corresponding dose of the complex without NAC.

by densitometry were expressed as % basal (lower part of the figure).

In an attempt to define the mechanism by which V(V)-Salsem induced ERK-phosphorylation, we examined the potential role of the oxidative and the mitogen activated protein kinase (MAPK) pathways. Osteoblasts were preincubated either with NAC (a free radical scavenger), Wortmannin (a phosphatidylinositol-3-kinase (PI3-K) inhibitor) or PD98059 (a mitogen extracellular kinase (MEK) inhibitor). Control experiments were also carried out with NAC, wortmannin, PD98059 and the vehicle (DMSO). Finally, 1 mM V(V)-Salsem was added for an additional hour and the activation of ERK was assessed as before. ERK-phosphorylation induced by V(V)-Salsem (1 mM) was totally inhibited by PD98059 and partially by wortmannin. On the other hand, NAC did not abrogate the V(V)-Salsem ERK-activation (Fig. 10).

In order to evaluate if ERK-1/2 activation may be involved in the antiproliferative effect of the vanadium complex, we tested again the effect of 100 μM of V(V)-Salsem plus PD98059 on cell proliferation. A slight but statistically significant ($p < 0.05$) reversion of the deleterious effect of the vanadium(V) complex on cell survival

could be determined for MC3T3-E1 cells with 1 μM PD98059 (Fig. 11). This reversion could not be detected for the tumoral osteoblasts. On the other hand, wortmannin was not able to reverse the deleterious effect of the complex. These results indicate that the ERK pathway is involved at least partly, in the V(V)-Salsem antiproliferative actions in the non-transformed osteoblasts like cells.

6. Discussion

Semicarbazone derivatives and vanadium species are pharmacologically active compounds both *in vivo* and *in vitro* systems [1,23,24]. Since these therapeutic properties can be modified by complexation, in the present study we have addressed the investigation of a complex of vanadium(V) with salicylaldehyde semicarbazone, V(V)-Salsem. The evaluation of its bioactivity and cytotoxicity is of particular interest.

Vanadium derivatives are a group of drugs with potential effects on hard tissues [2,36]. Bone is a dynamic tissue with a great capacity to remodel and repair throughout life [37]. The integrity of the skeleton depends on a series of events that regulate a coordi-

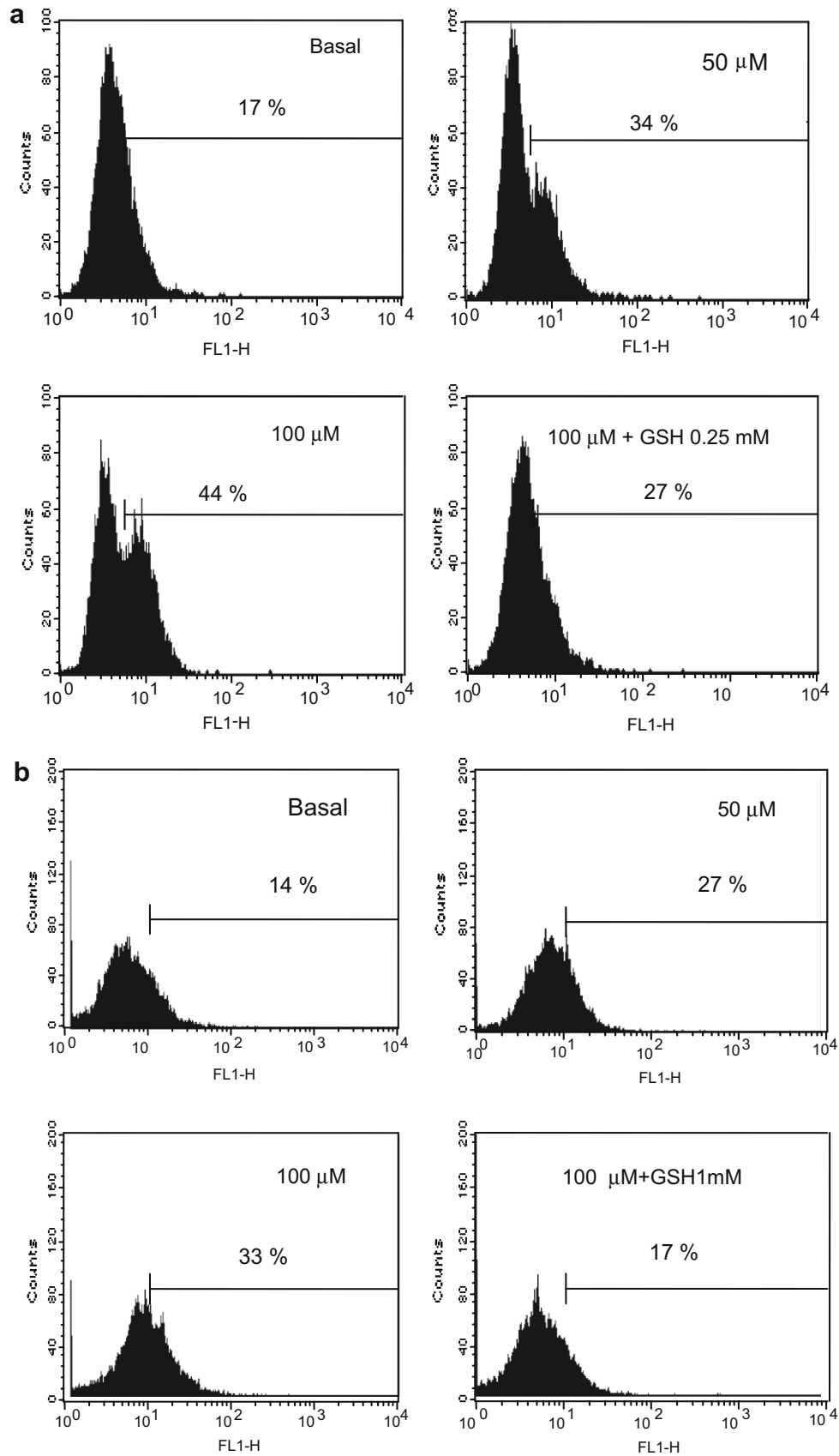


Fig. 9. (a) Effect of V(V)-Salsem on cellular apoptosis assessed by flow cytometry using Annexin V-FITC/PI. MC3T3-E1 cells were treated with 0 (basal), 50 μ M, 100 μ M of the complex and 0.25 mM of GSH plus 100 μ M of V(V)-Salsem for 24 h. Histograms are representative of three independent experiments. Number indicates of cells Annexin V-FITC positive. (b). Effect of V(V)-Salsem on cellular apoptosis assessed by flow cytometry using Annexin V-FITC/PI. UMR106 cells were treated with 0 (basal), 50 μ M, 100 μ M of the complex and 0.25 mM of GSH plus 100 μ M of V(V)-Salsem for 24 h. Histograms are representative of three independent experiments. Number indicates of cells Annexin V-FITC positive.

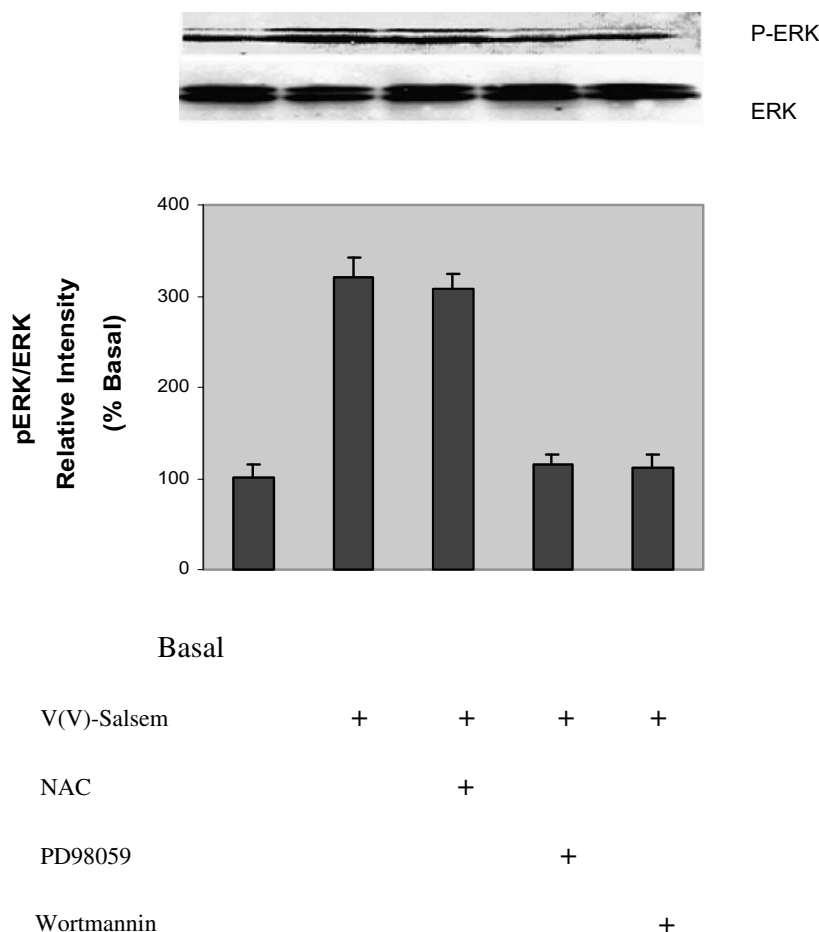


Fig. 10. Effect of V(V)-Salsem and inhibitors on ERK-1/2 activation. UMR106 osteoblast-like cells were preincubated either with PD98059 (50 μ M), NAC (1 mM), Wortmannin (10 μ M) for 1 h. Then, 1 mM of V(V)-Salsem was added for 1 additional hour. Relative intensity of stimulation corrected for total ERK-1/2 was determined by densitometry. Results are expressed as % basal and are representative of three independent experiments.

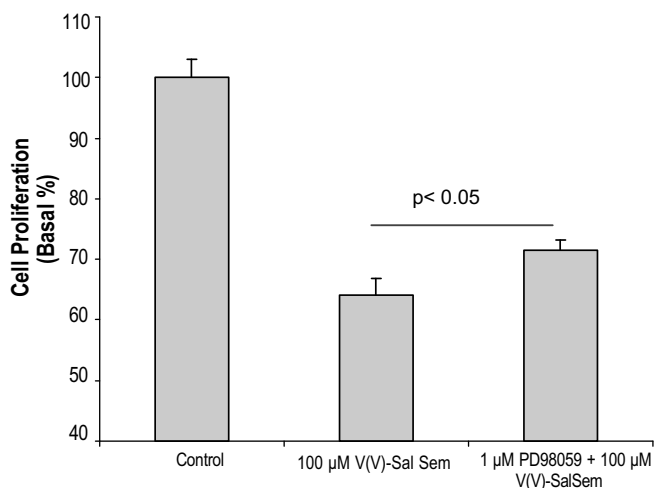


Fig. 11. Effect of V(V)-Salsem plus ERK-1/2 inhibitor, PD98059 on MC3T3-E1 osteoblast-like cells. Cells were preincubated either with 1 μ M of PD98059 for 30 min. prior the addition of the complex. Then, 100 μ M of V(V)-Salsem was added and the cells were incubated at 37 $^{\circ}$ C for 24 h. Results represent the mean \pm SEM ($n = 6$).

nated activity of osteoblasts and osteoclasts. In a model of normal and tumoral osteoblasts in culture, we found that vanadium(V) and vanadium(IV) species as well as different vanadium complexes

regulate cellular proliferation and differentiation [25,35,38,8,39]. In this osteoblast-like cells *in vitro* model, the results showed that the sensitivity of the non-transformed MC3T3-E1 cells to V(V)-Salsem induced cytotoxicity was greater than in the tumoral osteosarcoma cell line UMR106. Similar effects were previously reported by our group for other vanadium compounds [25,28,40,41]. Moreover, interesting pharmacological effects have also been published for vanadium derivatives of semicarbazones in different cellular lines [23,24]. In those studies, at 100 μ M, V(V)-Salsem caused a great cytotoxic effects on TK-10 (human kidney carcinoma) cells while other tumoral cell lines were less affected by this complex [24]. Together with our results, it can be seen that this complex exerted a deleterious effect on the human kidney carcinoma TK-10 and on the osteosarcoma UMR106 cell lines, being a good compound to be thoroughly explored in *in vivo* systems.

Several mechanisms have been proposed to explain the cytotoxicity of vanadium derivatives: morphological changes, cytoskeleton alterations, apoptosis, oxidative stress and ERK pathway activation [11,28,35,42,43]. The morphological alterations caused by V(V)-Salsem in the osteoblast cell lines displayed marked changes in the nuclear and cytoplasm characteristics. These changes are hallmarks of apoptosis and they are relatively stereotypical although there is much variation among the different cell types due to the numerous biochemical, functional and morphological peculiarities. The morphological changes in the cells were intensified in a dose response manner with great loss of cells and cellular structure at 100 μ M. Similar effects have been previously

reported by our group for other cell types in culture [44] as well as for other vanadium compounds [28,45]. On the other hand, some data from the literature have suggested that the cytotoxicity of vanadium may be responsible for the destruction of actin fibers [46,47]. The organization of the cytoskeleton is essential for many cellular functions. Actin fibers are one of the main components of cytoskeleton ubiquitously distributed in the cells. They determine the cellular shape and are involved in many cellular processes including signal transduction [48]. Changes in the cytoskeleton organization would likely lead to important consequences [43]. For these reasons, we next evaluated the effect of V(V)-Salsem on the actin cellular network. As it has been shown, also a dose-dependent-effect could be observed for the complex with again a greater disruption of actin fiber architecture in the non-transformed osteoblasts than in the tumoral ones.

These three deleterious effects of the complex (antiproliferative action, morphological alterations and actin cytoskeleton disruption) point to the cytotoxicity of V(V)-Salsem in osteoblast-like cells.

Moreover, in an attempt to elucidate the possible mechanism involved in the cytotoxicity of V(V)-Salsem, we evaluated the acute effect of the complex on the oxidative stress. It was assessed by the oxidation of the probe DHR 123 which mainly detects the intracellular level of the H_2O_2 [49–51]. Results showed an increase in ROS concentration as the cells were exposed to the complex. The increment in ROS levels correlated quite well with the antiproliferative effect observed in both cell lines.

Several studies have suggested that hydrogen peroxide is involved in vanadate-induced cell growth arrest and cell death [52–54]. Hence, if H_2O_2 is in fact related to the V(V)-Salsem induced cytotoxicity, the most likely alternative would be that the complex induced different intracellular levels of H_2O_2 depending on the cell line [52]. Besides, if this assumption was correct, one might expect a different sensitivity of MC3T3-E1 cells than in the tumoral osteoblasts to the addition of H_2O_2 to the cultures. Our results showed that although there is not a statistical difference in the intracellular levels in both cell lines, there is a greater sensitivity of the non-transformed cells in relation to the tumoral osteoblasts towards the H_2O_2 , as it could be established from the lower concentration of this agent able to cause a significant decrease in cell proliferation.

Other authors had previously suggested that certain antioxidants protect cells against ROS effects [55–58]. NAC, a well-known thiol-containing antioxidant, has had multiple clinical uses for more than 50 years [59,60]. The evidence from both *in vitro* and *in vivo* studies indicates that NAC is capable of facilitating intracellular GSH biosynthesis by reducing extracellular cystine to cysteine [61], or by supplying sulfhydryl (–SH) groups that can stimulate GSH synthesis and enhance glutathione-S-transferase activity [62]. Additionally, NAC is a potent free radical scavenger as a result of its nucleophilic reactions with ROS [63]. When NAC or a mixture of vitamins C and E were used in coincubations with the complex, the oxidative stress decreased in both cell lines. This effect could be seen through the cell proliferation assay which showed a partial amelioration of cell survival in the presence of ROS scavengers. Since scavengers could not reverse completely the damage caused by oxidative stress, other mechanisms were assumed to play a role in the complex cytotoxicity.

Apoptosis is considered a physiological mechanism of cell death, inherent to cellular development, which is triggered by different endogenous or exogenous factors [64]. These factors may be recognized by receptors in the cell surface and may cause a chain activation of cytoplasm proteins. As a consequence, a genetic program that leads to cell death is activated. This process is accompanied by characteristic morphological changes on the nucleus and the cytoplasm. Independently of the cellular type and the nature

of the trigger agent, the externalization of PS is always present in the earlier apoptotic events. Annexin V-FITC is a fluorescent probe with high affinity for PS allowing its determination by fluorometric assays. Our flow cytometry results showed an increment of the apoptotic cells over basal in the presence of V(V)-Salsem in both cell lines, but no necrotic cells could be determined. Similar results have been previously reported by other authors [33]. Secondary necrosis is probable the consequence of an apoptotic process in culture where no phagocytes are present to remove the dying cells. The secondary necrotic subpopulation could be hardly detectable, indicating that the loss of plasmatic membrane integrity by the apoptotic cell does not occur significantly under the presented conditions. Secondary necrosis may occur in a later stage of apoptosis. Since we measured this process in the adherent cell population, it is highly probable that the dying cells may have already detached from the surface of the dish and break into apoptotic bodies [33].

Apoptosis is associated in many cases with the generation of ROS, as it has been reported for a wide range of cells. Nowadays there are many unresolved questions concerning the relationship between apoptosis and the generation of ROS, such as which ROS are involved in apoptosis, what mechanisms and targets are important and whether apoptosis is triggered by ROS damage or if they are generated as a consequence of the cellular disruption that occurs during cell death [65]. It has been shown that vanadium-induced oxidative stress leads different cellular types to death by apoptotic and/or necrotic processes [11,66,67] as it was observed for V(V)-Salsem.

GSH, one important antioxidant in mammalian tissues, is one of the major detoxificant H_2O_2 scavengers [68,69]. Intracellular GSH level decreases during oxidative injury and it is an important parameter for the cellular redox status. For this reason and to obtain a better knowledge of the involvement of oxidative stress in the apoptosis caused by V(V)-Salsem, we analyzed the effect of 1 mM GSH added to the cultures. A beneficial effect dependent on GSH was determined in both cell lines as it has also been previously established for other cell lines [70].

The ERK pathway is classically recognized to play a key role in cell proliferation and differentiation [71]. Some investigations have shown that this pathway also mediates antiproliferation and cell death events [72]. Trying to get a better understanding of V(V)-Salsem cytotoxicity in osteoblasts, we studied the activation of ERK pathway in cultures incubated with the complex by the method previously described [73]. The complex caused the phosphorylation of ERK-1/2 in both cell lines.

Since the oxidative stress is also related to the activation of ERK pathway [74,75], we tried to elucidate its involvement in the complex induced cytotoxic effects in osteoblasts as it has been previously reported for vanadate [57,74]. To achieve this aim we have used NAC and specific inhibitors of ERK pathway. In the case of V(V)-Salsem, the role of oxidative stress in activating the intracellular signalling ERK cascade could not be determined. On the contrary, the specific inhibitors of ERK pathway (i.e. PD98059), caused a decrease in the phosphorylation of ERK. The evaluation of the proliferative actions of V(V)-Salsem in osteoblasts in culture in the presence of PD98059 demonstrated the implication of the ERK pathway activation in mediating the cytotoxic effects of the dioxovanadium(V) complex in the non-transformed osteoblasts. In fact, a partial compromise of this pathway, independent of the oxidative stress, seems to participate in the complex induced cytotoxicity.

All together, the results obtained in our model system suggest that the cytotoxicity of V(V)-Salsem in osteoblasts is mainly associated with the intracellular ROS overproduction. Besides, preliminary results obtained in our laboratory indicate that UMR106 cells have a higher basal concentration of GSH than MC3T3-E1 cells (data not shown). This difference in the basal GSH level could account, at least in part, for the lower cytotoxicity of the complex

in the osteosarcoma cells than in the non-transformed osteoblasts. Similar results were reported in Caco-2 cell system [76]. Moreover, a statistically significant negative correlation was found between cell survival and Rhodamine 123 fluorescence levels.

In conclusion, the cytotoxicity induced by V(V)-Salsem in the osteoblast-like cells is a complex phenomenon depending on several factors. An increase in the oxidative stress and the activation of ERK pathway possibly play a role in the morphological changes and in the survival of the cells. Besides, the results suggest that the phenotypic features of the cells and their mechanisms of antioxidant defense as well as the incidence of vanadium compound on the cytoskeleton organization also contributed to vanadium-induced cytotoxicity.

Acknowledgements

This work was supported by UNLP and CONICET (PIP 6366). D.A.B. and S.B.E. are members of the Carrera del Investigador, CONICET, Argentina. JR is a fellowship from CONICET, Argentina.

References

- [1] H. Beraldo, D. Gambino, *Mini Rev. Med. Chem.* 4 (2004) 31–39.
- [2] F.H. Nielsen, in: H. Sigel, A. Sigel (Eds.), *Metal Ions in Biological Systems, Vanadium and its Role in Life*, vol. 31, Marcel Dekker, New York, 1995, pp. 543–573.
- [3] R.K. Upreti, *Mol. Cell. Biochem.* 153 (1995) 67–171.
- [4] Y. Schechter, *Diabetes* 39 (1990) 1–5.
- [5] K.H. Thompson, J.H. McNeill, C. Orvig, *Chem. Rev.* 99 (1999) 2561–2571.
- [6] C. Djorjevic, in: H. Sigel, A. Sigel (Eds.), *Metal Ions in Biological Systems, Vanadium and its Role in Life*, vol. 31, Marcel Dekker, New York, 1995, pp. 595–616.
- [7] A.M. Evangelou, *Crit. Rev. Oncol. Hematol.* 42 (2002) 249–265.
- [8] A.M. Cortizo, M.S. Molinuelo, D.A. Barrio, L. Bruzzone, *Int. J. Biochem. Cell. Biol.* 38 (2006) 1171–1180.
- [9] D.A. Barrio, E.R. Cattáneo, M.C. Apezteguia, S.B. Etcheverry, *Can. J. Physiol. Pharmacol.* 84 (2006) 765–775.
- [10] S.B. Etcheverry, D.A. Barrio, in: K. Kustin, J. Pessoa, D.C. Crans (Eds.), *Vanadium: the Versatile Metal Chapter 15*, American Chemical Society, Washington DC, 2007, pp. 204–216.
- [11] M.S. Molinuelo, D.A. Barrio, A.M. Cortizo, S.B. Etcheverry, *Cancer Chemother. Pharmacol.* 53 (2004) 163–172.
- [12] M.J. Gresser, A.S. Tracey, in: N.D. Chasteen (Ed.), *Vanadium in Biological Systems*, Kluwer Academic Press, Dordrecht, 1990, pp. 63–79.
- [13] S.K. Pandey, J.F. Theberge, M. Bernier, A.K. Srivastava, *Biochemistry* 38 (1999) 14667–14675.
- [14] A.M. Cortizo, S.M. Kreda, in: J.A. Centeno, P.H. Coltery, G. Vernet, R.B. Finkelman, H. Gibb, J.C. Etienne (Eds.), *Metal Ions in Biology and Medicine*, vol. 6, Jhon Libbey, Eurotext, Paris, 2000, pp. 714–716.
- [15] J. Ye, M. Ding, S.S. Leonard, V.A. Robinson, L. Millecchi, X. Zhang, V. Castranova, V. Vallyathan, X. Shi, *Mol. Cell. Biochem.* 202 (1997) 9–17.
- [16] R.K. Narla, Y. Dong, D. Klis, F.M. Uckun, *Clin. Cancer Res.* 7 (2001) 1094–1110.
- [17] A.M. Mohamadin, L.A. Hammad, M. El-Bab, H.S. Abdel Gawad, *Basic Clin. Pharmacol. Toxicol.* 100 (2007) 84–90.
- [18] D.J. Reed, M.W. Fariss, *Pharmacol. Rev.* 36 (1984) 25–33.
- [19] H. Sakurai, *Environ. Health Perspect.* 3 (1994) 35–36.
- [20] S. Ivancsits, A. Pilger, E. Diem, A. Schaffer, H. Rüdiger, *Mutat. Res.* 519 (2002) 25–35.
- [21] J.L. Domingo, *Reprod. Toxicol.* 10 (1996) 175–182.
- [22] E. Sabbioni, G. Pozzi, S. Devos, A. Pintar, L. Casella, M. Fischbach, *Carcinogenesis* 14 (1993) 2565–2568.
- [23] P. Noblía, E.J. Baran, L. Otero, P. Draper, H. Cerecetto, M. Gonzalez, O.E. Piro, E. Castellano, T. Inohara, Y. Adachi, H. Sakurai, D. Gambino, *Eur. J. Inorg. Chem.* 2 (2004) 322–328.
- [24] P. Noblía, M. Vieites, B.S. Parajón-Costa, E.J. Baran, H. Cerecetto, P. Draper, M. Gonzalez, O.E. Piro, E.E. Castellano, A. Azqueta, A. Lopez de Cerain, A. Monge-Vega, D. Gambino, *J. Inorg. Biochem.* 99 (2005) 443–451.
- [25] A.M. Cortizo, S.B. Etcheverry, *Mol. Cell. Biochem.* 145 (1995) 97–102.
- [26] S.B. Etcheverry, D.C. Crans, A.D. Keramidás, A.M. Cortizo, *Arch. Biochem. Biophys.* 338 (1997) 7–14.
- [27] T. Okajima, K. Nakamura, H. Zhang, N. Ling, T. Tanabe, T. Yasuda, R.G. Rosenfeld, *Endocrinology* 130 (1992) 2201–2212.
- [28] V.C. Sállice, A.M. Cortizo, C.L. Gomez Dumm, S.B. Etcheverry, *Mol. Cell. Biochem.* 198 (1999) 119–128.
- [29] S.B. Etcheverry, E.G. Ferrer, L. Naso, D.A. Barrio, L. Lezama, T. Rojo, P.A.M. Williams, *Bioorg. Med. Chem.* 15 (2007) 6418–6424.
- [30] Y. Qin, M. Lu, X. Gong, *Cell. Biol. Int.* 32 (2008) 224–228.
- [31] H.J. Chae, J.S. Kang, J.L. Han, B.G. Bang, S.W. Chae, K.W. Kim, H.M. Kim, H.R. Kim, *Immunopharmacol. Immunotoxicol.* 22 (2000) 317–337.
- [32] M. Bradford, *Anal. Biochem.* 72 (1976) 249–254.
- [33] M. van Engeland, F.C. Ramaekers, B. Schutte, C.P. Reutelingsperger, *Cytometry* 24 (1996) 131–139.
- [34] E.K. Laemmli, *Nature* 227 (1970) 680–685.
- [35] D.A. Barrio, P.A.M. Williams, A.M. Cortizo, S.B. Etcheverry, *J. Biol. Inorg. Chem.* 8 (2003) 459–468.
- [36] M. Anke, B. Groppel, K. Gruhn, M. Langer, W. Arnhold, in: M. Anke, W. Baumann, H. Bräunlich, C. Brücker, B. Groppel, M. Grün (Eds.), *Sixth International Trace Element Symposium*, Schiller Universität, Jena, 1989, pp. 17–27.
- [37] A.J. Salgado, O.P. Coutinho, R.L. Reis, *Macromol. Biosci.* 4 (2004) 643–765.
- [38] E.G. Ferrer, M.V. Salinas, M.J. Correa, L. Naso, D.A. Barrio, S.B. Etcheverry, L. Lezama, T. Rojo, P.A.M. Williams, *J. Biol. Inorg. Chem.* 11 (2006) 791–801.
- [39] S.B. Etcheverry, E.G. Ferrer, L. Naso, J. Rivadeneira, V. Salinas, P.A.M. Williams, *J. Biol. Inorg. Chem.* 13 (2008) 345–447.
- [40] A.M. Cortizo, L. Bruzzone, M.S. Molinuelo, S.B. Etcheverry, *Toxicology* 147 (2000) 89–99.
- [41] J. Rivadeneira, D.A. Barrio, S.B. Etcheverry, E.J. Baran, *Biol. Trace Elem. Res.* 118 (2007) 159–166.
- [42] R.K. Narla, Y. Dong, F.M. Uckun, *Leuk. Lymphoma* 41 (2001) 625–634.
- [43] I. Osińska-Królicka, H. Podsiadly, K. Bukietyńska, M. Zemanek-Zboch, D. Nowak, K. Suchoszek-Lukaniuk, M. Malicka-Blaszkiewicz, *J. Inorg. Biochem.* 98 (2004) 2087–2098.
- [44] A.M. Cortizo, V.C. Sállice, C. Vescina, S.B. Etcheverry, *Biometals* 10 (1997) 127–133.
- [45] S.B. Etcheverry, D.C. Crans, A.D. Keramidás, A.M. Cortizo, *Arch. Biochem. Biophys.* 338 (1997) 7–14.
- [46] B. Lubber, S. Candidus, G. Handschuh, E. Mentele, P. Hutzler, S. Feller, J. Voss, H. Höfler, K.F. Becker, *Cell. Adhes. Commun.* 7 (2000) 391–408.
- [47] X.G. Yang, X.D. Yang, L. Yuan, K. Wang, D.C. Crans, *Pharm. Res.* 21 (2004) 1026–1033.
- [48] T.P. Stossel, *J. Biol. Chem.* 5 (1989) 18261–18264.
- [49] S. Szucs, G. Vámosi, R. Póka, A. Sárváry, H. Bárdos, M. Balázs, J. Kappelmayer, L. Tóth, J. Szöllosi, R. Adány, *Cytometry* 33 (1998) 19–31.
- [50] G. Rothe, A. Emmendorffer, A. Oser, J. Roesler, G. Valet, *J. Immunol. Methods* 138 (1991) 133–135.
- [51] A. Emmendorffer, M. Hecht, M.L. Matthes, J. Roesler, *J. Immunol. Methods* 131 (1990) 269–275.
- [52] M.A.M. Capella, L.S. Capella, R.C. Valente, M. Gefé, A.G. Lopes, *Cell. Biol. Toxicol.* 23 (2007) 413–420.
- [53] C. Huang, Z. Zhang, M. Ding, J. Li, J. Ye, S.S. Leonard, H.M. Shen, L. Butterworth, Y. Lu, M. Costa, Y. Rojanasakul, V. Castranova, V. Vallyathan, X. Shi, *J. Biol. Chem.* 275 (2000) 32516–32522.
- [54] M. Torres, H.J. Forman, *Ann. NY Acad. Sci.* 973 (2002) 345–348.
- [55] J. Ye, M. Ding, S.S. Leonard, V.A. Robinson, L. Millecchia, X. Zhang, V. Castranova, V. Vallyathan, X. Shi, *Mol. Cell. Biochem.* 202 (1999) 9–17.
- [56] X. Yin, A.J. Davidson, S.S. Tsang, *Mol. Cell. Biochem.* 115 (1992) 85–96.
- [57] Z. Zhang, H. Chuanshu, J. Li, S.S. Leonard, R. Lanciotti, L. Butterworth, X. Shi, *Arch. Biochem. Biophys.* 392 (2001) 311–320.
- [58] C. Huang, M. Ding, J. Li, S.S. Leonard, Y. Rojanasakul, V. Castranova, V. Vallyathan, G. Ju, X. Shi, *J. Biol. Chem.* 276 (2001) 22397–22403.
- [59] S. Parcell, *Altern. Med. Rev.* 7 (2002) 22–44.
- [60] R.J. Flanagan, T.J. Meredith, *Am. J. Med.* 91 (1991) 1315–1395.
- [61] R.D. Issels, A. Nagele, K.G. Eckert, W. Wilmanns, *Biochem. Pharmacol.* 37 (1988) 881–888.
- [62] N. De Vries, S. De Flora, *J. Cell. Biochem. Suppl.* 17F (1993) S270–S277.
- [63] O.I. Arouma, B. Halliwell, B.M. Hoey, J. Butler, *Free Radical Biol. Med.* 6 (1989) 593–597.
- [64] F. Silvestri, D. Ribatti, B. Nico, N. Silvestri, A. Romito, F. Dammacco, *Ann. Ital. Med. Int.* 10 (1995).
- [65] G.G. Perrone, S.X. Tan, I.W. Dawes, *Biochim. Biophys. Acta* 1783 (2008) 1354–1368.
- [66] M. Caicedo, J.J. Jacobs, A. Reddy, N.J. Hallab, *J. Biomed. Mater. Res. A* 86 (2008) 05–13.
- [67] P.S. Chien, O.T. Mak, H.J. Huang, *Biochem. Biophys. Res. Commun.* 339 (2006) 562–568.
- [68] M.G. Baigi, L. Brault, A. Néguesque, M. Beley, R.E. Hilali, F. Gaüzère, D. Bagrel, *Toxicol. In Vitro* 22 (2008) 1547–1554.
- [69] M. Naziroglu, A. Lückhoff, *J. Neurol. Sci.* 270 (2008) 152–158.
- [70] L.S. Capella, M.R. Gefé, E.F. Silva, O. Affonso-Mitidieri, A.G. Lopes, V.M. Rumjanek, M.-A. Capella, *Arch. Biochem. Biophys.* 406 (2002) 65–72.
- [71] Y.Z. Wang, J.C. Bonner, *Am. J. Respir. Cell. Mol. Biol.* 22 (2000) 590–596.
- [72] C. Blazquez, I. Galve-Roperh, M. Guzmán, *FASEB J.* 14 (2000) 2315–2322.
- [73] F. D’Onofrio, M.Q. Le, J.L. Chiasson, A.K. Srivastava, *FEBS Lett.* 340 (1994) 269–274.
- [74] J.H. Park, E.J. Kim, H.-Y. Jang, H. Shim, K.K. Lee, H.J. Jo, H.J. Kim, S.H. Yang, E.T. Jeong, H.-R. Kim, *Oncol. Rep.* 20 (2008) 379–384.
- [75] Y. Lu, A. Cederbaum, *Free Radical Biol. Med.* 43 (2007) 1061–1075.
- [76] C. Giovannini, B. Scazzocchio, P. Matarrese, R. Vari, M. D’Archivio, R. Di Benedetto, S. Casciani, M.-R. Dessi, E. Straface, W. Malorni, R. Masella, *J. Nutr. Biochem.* 19 (2008) 118–128.